Pure & Appl. Chem., Vol 56, No. 12, pp 1703-1714, 1984.
Printed in Great Britain.

0033-4545/84 $3.00 + 0.00
Pergamon Press Ltd.

THE CHEMISTRY OF CERAMIC GRAIN BOUNDARIES

W. D. Kingery

Department of Materials Science and Engineering, Massachusetts Institute of Technology, Cambridge, Massachusetts 02139, USA

Abstract - The arrangement of ions and grain boundary structures in ceramics have been made clearer by high resolution electron microscopy and computer simulations. Oxide grain boundaries are more open than metal boundaries. Calculations indicate that there are at least some low energy sites for all solutes. Widespread segregation at boundaries and boundary chemistry different from the bulk is thus expected; it is experimentally found to be the case. Boundaries in ceramic oxides generally have an electrical charge and associated space charge region which also affect boundary chemistry. Many properties of ceramics are affected by boundary chemistry and boundary charge.

The application of chemistry to ceramic materials has mostly been focussed on developing and understanding the composition and structure of each of the phases present and how they developed. This provides the essential basis for ceramic studies of how the arrangement of these phases, the microstructure, develops and how that microstructure affects and controls ceramic properties. It is increasingly being recognized that the boundary region between grains is an essential constituent of the microstructure. The composition and structure--the chemistry, if you like--of the grain boundary region must be a necessary constituent of the further development of high technology ceramics.

In the last few years both experimental techniques and theoretical methods have been developed which make it practical to investigate the chemistry of the boundary regions in a way that has not heretofore been possible. It is my purpose to discuss a few of these recent developments to illustrate how this new field of chemistry is being nucleated and its importance for the continuing development of modern ceramics.

GRAIN BOUNDARY STRUCTURE

Any understanding of grain boundary chemistry must ultimately depend on knowing the arrangement of ions in the boundary and the existence of dislocations and point defects in the boundary structure. In forming an arbitrarily oriented grain boundary between two crystals, one can imagine adjusting the position of the crystals adjoining the boundary, describing the orientation of the boundary plane, allowing translation of the crystals to their minimum relative energy positions and letting the atoms in and near the boundary relax to a minimum total energy. This requires eight macroscopic parameters to define a particular boundary, and it is clear that the specification of boundary structure is a complex problem in the general case. This difficulty is accentuated by the fact that most information about detailed boundary structures has been developed from computer simulation studies applied principally to metals and that most have pertained to special grain boundaries with structures having relatively short wavelength periodicity (1-5).

Our present view and description of boundary structures are largely based on Bollmann's O-lattice theory (6,7). At particular orientations, special low-energy boundaries occur in which there is a significant periodic structure that can be described locally with ordered arrays of compact polyhedra (8-10). These can be classified as having coincident site lattice matching in which the two adjacent crystals have a fraction of their atoms located on the three-dimensional coincident site lattice. Or, they may be described in terms of near coincident site lattice matching, in which a two-dimensional matching is achieved across a boundary plane with the inclusion of a network of grain boundary dislocations (11). Experimental observations with gold and germanium have shown these characteristics (12,13). Recent studies in magnesium oxide (14) and in aluminum oxide (15) make it clear that boundaries of these ionic materials with crystal misorientations near those corresponding to special boundaries of low energy do indeed consist of areas of special boundary, plus arrays of grain boundary dislocations (14,15). Faceted boundaries that are presumed to be

of low energy orientation are observed in a number of oxide ceramics (16). In aluminum oxide, at least, it has been found that the primary plane adopted by special boundaries tends to contain the highest number of coincident lattice sites (15).

During the past several years, computer simulation programs have been developed which allow the modeling of coincident grain boundary structures in oxides using an atomistic simulation technique (17-22). Results of one calculation for the relaxed structure of a 36.9°, Σ-5, (310)/[001] tilt boundary is illustrated in Fig. 1. A significant result is that this

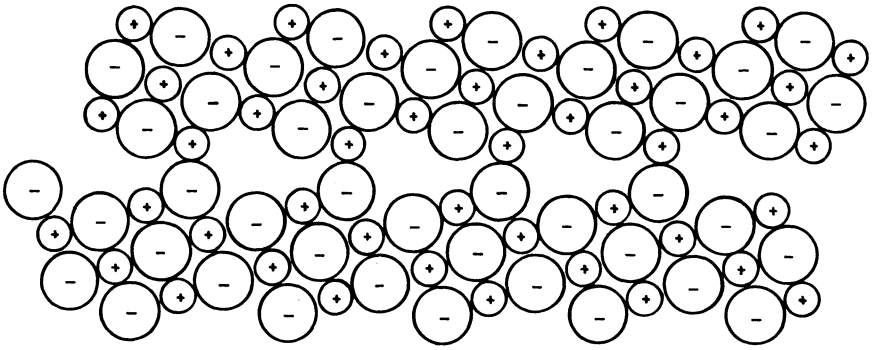

Fig. 1. Relaxed structure of the 36.9° (310)/[001] tilt boundary in NiO or MgO drawn with Pauling's ionic radii. The structure is more open than equivalent boundaries in metals (22).

configuration is much less dense than that of the corresponding grain boundary in metals (7,23). The structure can be resolved into an array of [100] dislocations. Similar results are found for other tilt boundaries. Boundary energy minima are found at the coincident site lattice orientations, in accord with experimental observations. In contrast, calculations of <001> coincident twist boundaries in MgO and NiO (17) did not lead to stable structures. More recent calculations (21,22) have found that starting with an anti-coincidence configuration with like ions facing each other across the boundary, other ions are quite close to ions of the opposite charge. If the anti-coincidence ions in one plane are removed and the remaining ions relaxed to an equilibrium structure, a stable boundary results. That is, the introduction of Schottky defects into the boundary structure reduces the interfacial energy and leads to boundary stability. Thus, it seems that in both tilt and twist boundaries an open structure is stable.

Utilizing electron diffraction techniques and modeling the structure of a (001) twist boundary as a thin crystal having a width in which there is a uniform interplanar spacing slightly larger than the spacing in the perfect crystal, it is possible to determine these characteristics. For twist boundaries of gold (24) and NiO (25) with the same misorientation angle, 22°, it is found that the measured boundary width in nickel oxide is somewhat less than gold, but that there is a substantially larger increase in the plane spacing in the oxide material as compared with the metal, as illustrated in Table 1.

TABLE 1. Structural data from (001) twist boundaries obtained by electron diffraction (25).

	Ag	NiO
Misorientation angle	22°	22°
Boundary width	9±4Å	5±1Å
Increase in boundary plane spacing	5±3%	15±5%

These experimental results reinforce the theoretical calculations with regard to the more open structure of oxide grain boundaries as compared with metals.

Detailed calculations of structure and experimental diffraction studies are presently limited to the more simple structures of coincidence boundaries. However, random boundaries can be described in terms of combination of special boundary structures (8-10,11), and the

open structure of the special coincident site lattice boundaries in oxides suggest there may not be so much difference as one might expect. Recent experimental measurements of the relative segregation of calcium and silicon on special and nonspecial boundaries in MgO (26) are shown in Table 2. While there is significantly more segregation at the nonspecial boundary, it is only a factor of two. Thus, for our first order evaluations we should probably focus on the similarity of boundaries in ceramic oxides.

TABLE 2. Relative concentrations of Ca and Si segregated at special and nonspecial twist boundaries in MgO at 1375°C (26).

Boundary	Ca (wt%)	Si (wt%)
36.9° (Σ 5)	0.42	0.43
28.5° (Σ 17)	0.46	0.49
24.2° -	0.91	0.71

GRAIN BOUNDARY CHEMISTRY

Solutes that lower the interface energy relative to the bulk phase decrease the free energy of the system by being concentrated at the interface. For dilute solution one anticipates and finds an adsorption confined to one or a few monolayers. The tendency for segregation to occur in a narrow region is illustrated in Fig. 2 where Auger electron spectroscopy results for calcium, silicon and surface carbon adsorption at MgO boundaries (27) are plotted together with data for a number of metals (28). The result is precisely what one would expect from the statistics of sputtering if all the solute atoms are situated at the grain boundary plane, although some caveats are required with regard to sputtering yields.

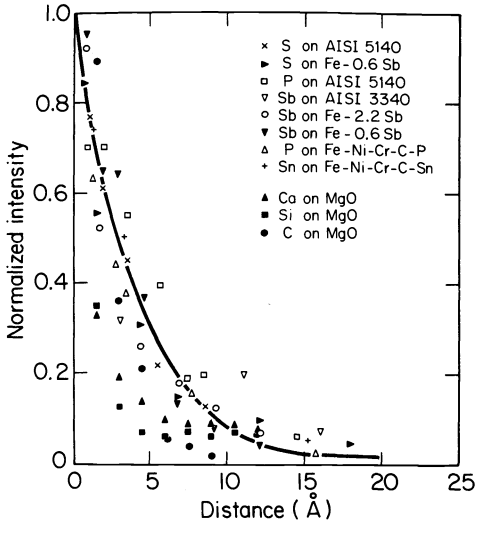

Fig. 2

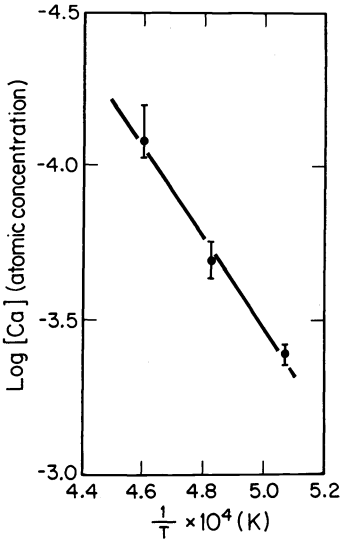

Fig. 3

Fig. 2. Normalized intensity of Auger electron signal with distance into a grain boundary fracture surface (27,28).

Fig. 3. Exponential temperature dependence of calcium segregation in Al_2O_3. (30).

The simplest sort of adsorption theory is that of a Langmuir type where there is a single layer of a single adsorbate and no site-to-site interactions. This theory was applied to grain boundary segregation by McLean (29). For dilute solutions,

$$C_B = \frac{C_\infty \exp -(\Delta G_I/kT)}{1 + C_\infty \exp -(\Delta G_I/kT)} \quad (1)$$

where C_B is the fraction occupation of grain boundary sites and C_∞ is the bulk concentration and ΔG_I is the free energy of interaction between the solute ion and the boundary. More complicated monolayer and multilayer expressions reduce to this form in the case of dilute solutions. Experimental results for calcium oxide in alumina (30) and of alumina in silicon carbide (31) are of this form, as illustrated in Fig. 3.

Segregation at boundaries in oxide and carbide materials is extensive. As illustrated in Fig. 4, a sample of magnesium oxide with impurities of aluminum, silicon, calcium and titanium has grain boundaries in which each of these solutes is present in significant amounts. Similarly, in aluminum oxide extensive boundary segregation occurs, as illustrated in Fig. 5. In addition to these and other data for aluminum oxide and magnesium oxide, CaO is found to concentrate at boundaries in magnesium zinc ferrite, as do SiO_2 and TiO_2 (34, 35). Calcium has been found segregated at boundaries in sodium β-alumina (36). Lithium oxide has been found segregated at grain boundaries of zinc oxide (37) and nickel oxide (38). Potassium and calcium have been found segregated at the surface of TiO_2 (39) and bismuth is known to segregate at boundaries in zinc oxide (40). Iron segregates at boundaries in barium titanate (41). It seems likely that a large part of the segregation of iron, chromium and scandium adjacent to grain boundaries in MgO (42,43) and of titania in aluminum oxide (33) is related to the boundary space charge discussed in the next section.

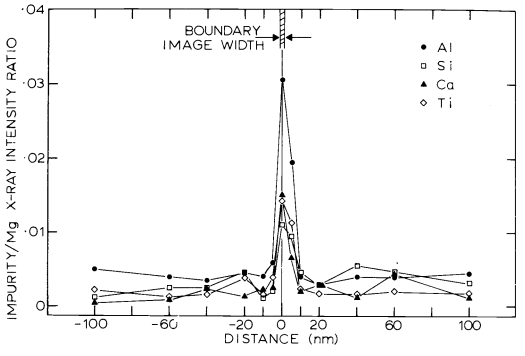

Fig. 4

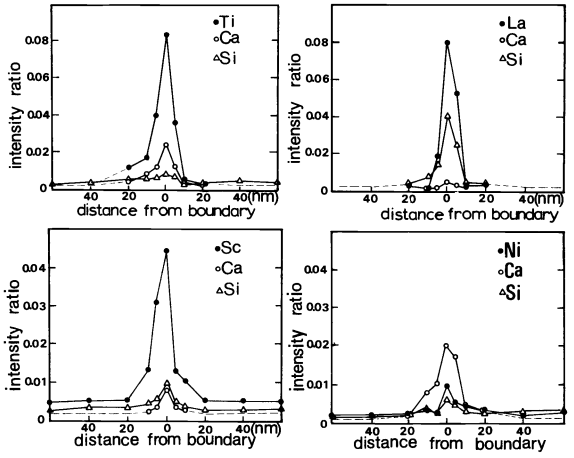

Fig. 5

Fig. 4. Boundary segregation of aluminum, silicon, calcium and titanium in MgO (32).

Fig. 5. Boundary segregation of Ti, La, Sc, Ni, Ca and Si in Al_2O_3 (33).

In ionic materials, solutes segregate to grain boundaries to relieve solute strain energy which is lower at the grain boundary than in the bulk. This is most important for solutes having an ionic radius significantly different from the lattice ions. In addition to the size effect, however, there is a spread in the Madelung potentials of the sites near the grain boundaries in ionic crystals such that some sites are favorable for any aliovalent impurity ion. Using the relaxed structures of coincidence symmetry boundaries in nickel oxide, Duffy and Tasker (44) have calculated the difference in energy of introducing a solute ion into the bulk and into the grain boundary structure. The most favorable sites were selected by inspection and the lowest substitutional energies for each impurity determined. The calculated interaction energies varied appreciably for different boundaries, as illustrated in Table 3. However, for every solute and boundary at least some sites were found which are favorable for any solute ion of different atomic radius or charge from the host.

TABLE 3. The interaction energies of impurities at coincident tilt boundaries in NiO. The interaction energy is defined as the difference between the substitutional energies at the boundary and at the bulk. (Duffy and Tasker (44)).

	Interaction Energies (eV) Impurity		
Boundary	$Co_{Ni}2+$	$Al_{Ni}2+$	$Ce_{Ni}2+$
(310)/[001]	-0.09	-0.17	-1.15
(320)/[001]	-0.22	-0.39	-1.73
$(2\bar{1}1)/[001]$	-0.12	-0.24	-0.41
$(1\bar{2}2)/[001]$	-0.07	-0.53	-0.74

For the $(2\bar{1}1)/[011]$ tilt boundary in NiO, the interaction energies of a series of ions of

different ionic radius have been calculated and are shown in Table 4. The interaction energy increases with the increasing radius and this is the predominant factor determining the interaction energy, as illustrated for the case of Ce^{4+}. For a bulk concentration of 10^{-4} and a temperature of 1000 K, the relative boundary concentrations are calculated from Eq. 1, ignoring entropy terms. For ions with a substantially different ionic radius from the host lattice, it is seen that the low energy boundary sites are saturated.

TABLE 4. Interaction energies (U_I) of isovalent impurities at the $(2\bar{1}1)/[011]$ tilt boundary in NiO, with the corresponding boundary impurity concentrations for $C_\infty = 10^{-4}$ and T = 1000 K. (Duffy and Tasker (44)).

Impurity Ion	Ionic Radius (Å)	Interaction Energy (eV)	$C_B = \frac{C_\infty e^{-U_I/kT}}{1+C_\infty e^{-U_I/kT}}$
Mg^{2+}	0.722	-0.100	3.2×10^{-4}
Co^{2+}	0.745	-0.118	3.94×10^{-4}
Fe^{2+}	0.771	-0.247	1.76×10^{-3}
Ce^{4+}	0.80	-0.41	1.2×10^{-2}
Mn^{2+}	0.836	-.488	2.83×10^{-2}
Ca^{2+}	1.021	-1.185	0.990
Sr^{2+}	1.196	-2.148	1.00
Ba^{2+}	1.377	-3.376	1.00

The substitutional energy of a solute ion with a radius different from the host ion radius, that is the strain energy for the ion introduced in a lattice, U_o, is usually taken as proportional to the square of the difference between radii after Eshelby (45):

$$U_o = \frac{6\pi r^3 \left(\frac{\Delta r}{r}\right)^2 B}{[1 + 3B/4\mu]} \qquad (2)$$

where Δr is the size misfit of the solute, B is the bulk modulus of the solute and μ the shear modulus of the matrix. The calculations of Duffy and Tasker gave something more like a linear relationship than $(\Delta r)^2$ and suggested that the alternative approach of considering the interaction between the dilation or volume change introduced by the solute with the hydrostatic stress field of the boundary might be appropriate. Following derivations of Cottrell (46) and Webb (47) for interactions with dislocations and low-angle tilt boundaries, segregation should have a linear variation with misfit radius for small values. Actually, the interaction energies calculated by Duffy and Tasker seem intermediate between these relationships, but are in good agreement with a first power relationship for small values of misfit.

Li and Kingery have studied the relative segregation of several solutes on clean precipitation-free boundaries, finding that the boundary segregation depended in large part on the ionic radius misfit, as illustrated in Fig. 6. When plotted as estimated concentrations, their data are intermediate between a first power and second power relationship.

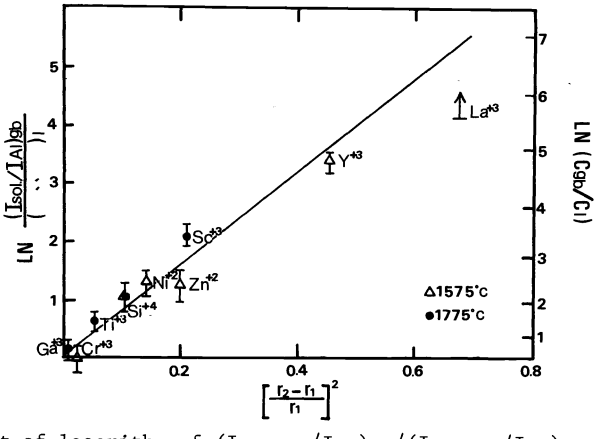

Fig. 6. Plot of logarithm of $(I_{solute}/I_{Al})_{gb}/(I_{solute}/I_{Al})_\ell$ vs $(r_2-r_1/r_1)^2$ for divalent and trivalent solutes in Al_2O_3.

Another feature of grain boundary chemistry which has not been much investigated is the likelihood of interband energy states and unusual oxidation states such as are found at surfaces. Surface photovoltage spectroscopy has shown the existence of interband surface states in cadmium sulfide (48) and zinc oxide (49,50). Surface states equivalent to Ti^{3+} and excess electrons in TiO_2 (51,52) and surface structures equivalent to Al_2O or AlO at the surface of Al_2O_3 (53) have been described along with interband energy levels in TiO_2 and TiO_2-hydroxyl services (54). Recent deep-layer capacitance studies of ZnO containing Bi_2O_3 and CoO in solution show definite energy levels in the band gap that may be associated with zinc vacancies (55). There seems no reason not to expect the existence of "surface states" at the grain boundaries of ceramic oxides which will have an influence on their stability and characteristics.

Data and analyses for multiple solutes, which are usually the case for ceramics, have not been much evaluated. If we have two solutes whose only driving force for segregation is the strain energy from Eq. 1 we can write

$$\frac{C_{B_2}}{C_{B_1}} = \frac{C_{\infty_2}}{C_{\infty_1}} \exp\left[-(\Delta G_{I_2} - \Delta G_{I_1})/kT\right] \tag{3}$$

which indicates that the relative boundary concentrations of two solutes may be very different indeed from the concentrations in the bulk.

ASSOCIATED SPACE CHARGE REGION

In a sufficiently pure material, an intrinsic electric boundary charge arises from localized surface states for charged ions and for electrons having energies different from the bulk, as well as charged vacancies which have energies different from the bulk. However, resulting boundary compositions, stoichiometry, and electric charge are a strong function of the chemical composition, boundary orientation, heat treatment, and it is doubted that intrinsic defects have been observed at grain boundaries in ceramic materials. A general random grain boundary contains many steps and kinks which can act as sources and sinks for vacancies and be represented as equivalent to two free surfaces back-to-back (56). If it is assumed that such grain boundaries act as infinite sources and sinks for vacancies with an innate free energy of formation independent of the type of boundary, then the requirement for charge neutrality in the bulk gives rise to a boundary charge and an associated space charge region. Aliovalent ions in solution affect the vacancy concentrations in the bulk and thus the electric charge on the boundary (56-60). However, the assumption that the energy required to form vacancies is independent of the nature of the boundary or its chemical composition is surely too simple.

Duffy and Tasker (61) have used computer simulation techniques to calculate the formation energies of intrinsic defects near coincidence grain boundaries in nickel oxide. While coincidence boundaries do not have kinks and steps, they do have low energy defect sites associated with the boundary structure such that the concentration of defects can be enhanced at the boundary; this results in a net charge density with which a space charge layer will be associated. Several possible defect sites at a given boundary were selected by inspection and the energy calculated relative to the bulk crystal. For each defect studied, at least some lower energy sites at the boundary than in the bulk were determined. The lowest interaction energies, i.e., boundary energy less the bulk energy, were determined for cation vacancies, anion vacancies and holes (associated with a nickel ion), as shown in Table 5. In each case, the interaction energy corresponds to a substantial enhancement of cation vacancies and holes at the boundary. In every case, the cation vacancy interaction energy is greater than that for the hole so it is calculated that a negative boundary with excess concentration of cation vacancies results.

TABLE 5. Interaction energies of intrinsic defects at coincident tilt boundaries in NiO. The lowest energy sites were chosen for each defect (61).

Interaction Energies (eV)		
Cation Vacancy	Anion Vacancy	Hole (Ni^{3+} Ion)
-0.36	-0.30	-0.25
-1.61	-1.25	-0.45
-0.95	-0.98	-0.23
-1.54	-1.56	-0.54

The overall electrical charge at the boundary will result from multiple effects related to the interaction energy of defects between the bulk and boundary, the influence of added solutes on bulk and boundary defect concentration, and elastic field interactions leading to boundary segregation of charged ions. The combined interactions have been discussed by Yan, Cannon and Bowen (62) and by Duffy and Tasker (61).

The boundary charge is accompanied by an associated space charge layer for which theory has been independently developed as the Guoy-Chapman diffuse double layer for ionic solutions (63-64), for semiconductors (65), and for ionic crystals (57-60) with equivalent results. If thermal equilibrium is achieved and the potential at the surface is given as ψ_o, the interaction between charges in the system is determined by Poisson's equation and the distribution of charged ions in the solution is determined by a Boltzmann expression such that for a planar boundary with particles of charge (ze) and a characteristic Debye length ($\chi_D = (\varepsilon kT/8\pi(ze)^2 n)^{\frac{1}{2}}$) where ε is the dielectric constant and n is the number of charged particles per cm^3 far from the surface, the electrical potential distribution in the space charge layer is given by

$$\frac{ze\psi}{kT} = 2\ \ln\frac{1+e^{-x/xD}[(e^{ze\psi_o/2kT}-1)(e^{ze\psi_o/2kT}+1)]}{1-e^{-x/xD}[(e^{ze\psi_o/2kT}-1)(e^{ze\psi_o/2kT}+1)]} \qquad (4)$$

This result corresponds to an exponential decrease in the potential over a characteristic length proportional to the inverse square root of the concentration of the principal charge-carrying species far from the boundary. These equations do not consider the finite dimensions of the mobile charges. While this is not much of a problem for very dilute solutions, it causes essential difficulties for the more concentrated solutions typical of ceramic materials where calculated charge concentrations near the interface become physically untenable. Stern (66) divided the charge layer into two parts, one thought of as ions absorbed to the wall corresponding to a surface charge concentration in a plane at a small distance Δ from the surface charge on the wall, where Δ is assumed to be of atomic dimensions and the fraction of the charge concentrated in the Stern layer depends on temperature in a way analogous to the Langmuir absorption isotherm. The Stern representation is obviously still a very simplified picture.

The ionic radius of scandium is very close to that of magnesium, such that the strain energy term leading to segregation is small. For a sample containing some silicon and calcium which are segregated in the plane of the grain boundary, sputter profiles determined by Auger spectroscopy give a quite different result for the Sc^{+3} corresponding to its location in the space charge region, providing charge composition for the boundary layer (Fig. 7).

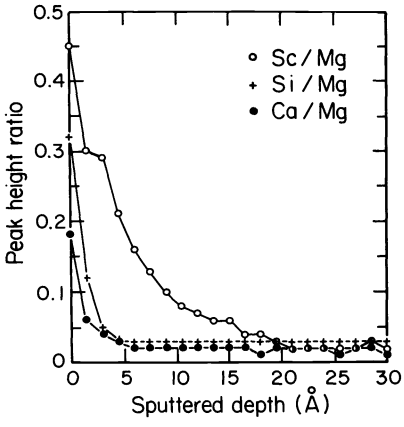

Fig. 7. The ratios Sc/Mg, Si/Mg, and Ca/Mg in the sputter profile of grain boundary site in vacuum-fractured polycrystalline MgO containing 3000 cation ppm Sc.

In this sample, which contained 3,000 cation ppm scandium, the approach of space charge ions to the boundary is apparently more constrained than predicted by either continuum theory. It was considered appropriate to evaluate a multiple layer adsorption approach in which the free energy of adsorption was considered to vary with the electrostatic potential. The electrostatic potential at each absorbed layer beyond the first decreases as a function of the $Sc_{Mg}^{\cdot}$ concentration in previous layers, since they partially compensate the boundary charge. This situation may perhaps be likened to potential-dependent adsorption of ions at

an electrode in an electrolytic solution. The result is shown in Fig. 8, and apparently provides a better approximation of the observed segregation behavior, even though it still represents a greatly oversimplified picture.

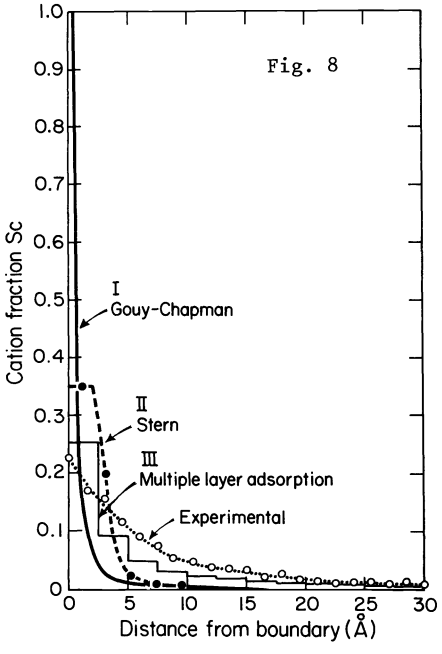

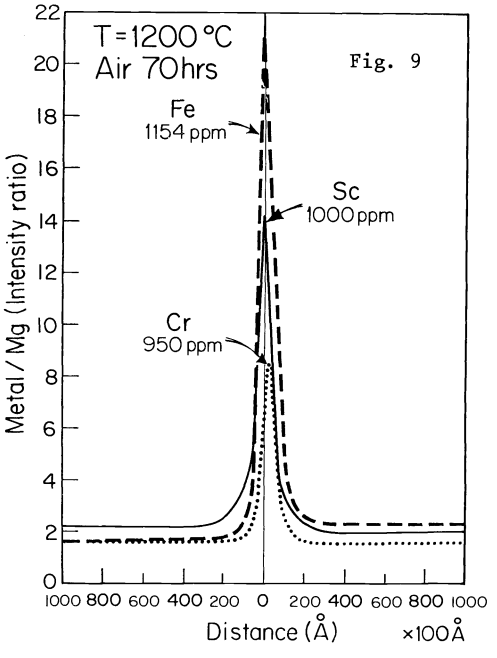

Fig. 8. Experimentally observed Sc segregation profile, Sc segregation profiles calculated from the Gouy-Chapman and Stern solutions for the space charge potential, and multiple-layer adsorption approximation, as described in the text.

Fig. 9. Segregation of Cr^{3+}, Sc^{3+} and Fe^{3+} to an MgO boundary.

The segregation to grain boundaries in MgO of Fe^{3+} and Cr^{3+} is similar to that for scandium and presumably also results from accumulation in the space charge region (Fig. 9). Li and Kingery found a larger concentration of Ti^{4+} at grain boundaries in Al_2O_3 than could be accounted for on the basis of strain energy and concluded that this was related to space charge accumulation.

The influence of concentration on segregation at boundaries and the space charge region has been evaluated for scandium, iron and chromium in MgO (67), as shown in Fig. 10. Up to concentrations of 1,000 ppm there is a linear relationship for the scandium and iron, but chromium shows a decrease which is believed to result from the association of chromium ions with negatively charged cation vacancies. The general effect of defect association and resulting dipole contributions to solute segregation are discussed by Yan, Cannon and Bowen (62).

BOUNDARY PHASES

As has been illustrated in Fig. 3, the degree of segregation increases as the temperature is lowered, which requires relatively fast cooling to freeze in an equilibrium situation at high temperature. As shown in Fig. 11, samples slow cooled from 1500°C show an increase in iron segregation at a boundary in MgO as compared with samples air quenched.

More important effects occurring during heat treatment are related to the limited solubility at lower temperatures such that precipitates form. These usually first appear at the grain boundaries since the accommodation of strain energy reduces the nucleation barrier. Magnesium ferrite equilibrium phase separation can be observed in MgO at temperatures as low as 770°C (68), and phase separation in the NiO-CoO system has been observed at 650°C (69). The solubilities of SiO_2 and ZrO_2 in MgO are small, less than 0.00008 mole fraction for ZrO_2 at 1850°C (70). The solubility of Al_2O_3 is only 0.0004 mole fraction at 1200°C in MgO. A whole range of different morphologies of precipitates occur, often as fine particle size constituents that require electron microscopy for their observation.

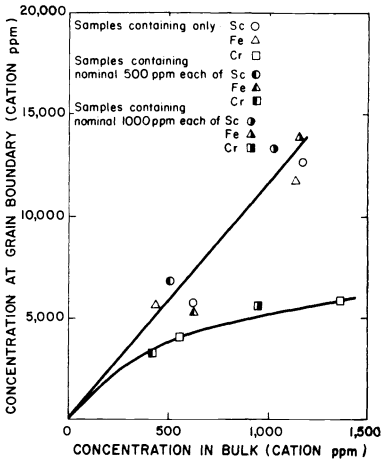

Fig. 10

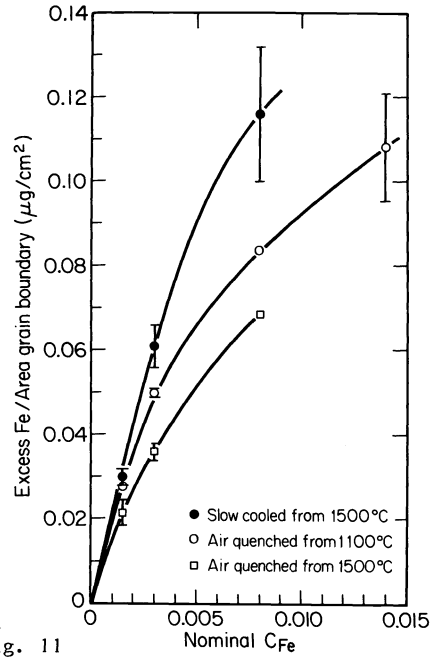

Fig. 11

Fig. 10. Concentration dependence of boundary segregation of iron, scandium and chromium in MgO (63).

Fig. 11. Influence of concentration of iron in MgO, and of the cooling rate, on observed boundary segregation.

The distribution of the boundary phases tends to be highly nonuniform and has led to a certain amount of confusion. In zinc oxide, for example (55), at temperatures above the eutectic temperature there is a continuous liquid phase which wets all of the boundaries and is responsible for the densification process in commercial materials. If a sample is rapidly quenched from this temperature region, that feature of the microstructure can be readily observed. However, if a sample is slowly cooled, there is a decrease in the amount of liquid phase present and also a change in the dihedral angle for typical boundaries, as illustrated in Fig. 12. This change in dihedral angle corresponds to an important change in the second phase distribution. Instead of covering the faces, the second phase retracts to the joins between three grains and, with further equilibration, becomes droplets at four grain intersections. As a result, boundary characteristics depend very strongly on the heat treatment, annealing schedule and rate of cooling. Even with very slow cooling, some boundary orientations with low energy configurations persist with a liquid phase present after slow cooling. These low energy boundary phase configurations frequently have ledged interfaces, sometimes with precipitate particles present as well as an amorphous phase; such structures have been observed for a variety of compositions.

APPLICATIONS IN CERAMICS

In the last ten years, as the tools for observing the characteristics of grain boundaries in polycrystalline ceramic materials have developed along with the capability for chemical analysis and microstructure determination, the recognition of their importance for ceramic properties has grown. Silicon carbide is a semiconductor material; with additions of beryllia, which segregate to the boundaries, it can be used as a high thermal conductivity material of good electrical resistivity. Usual silicon carbide powders cannot be sintered at high temperatures,but the addition of a bit of carbon together with a small amount of boron and aluminum affects the surface and grain boundary properties in such a way that dense ceramics can be manufactured from what previously was considered an "unsinterable" material. The resultant high temperature properties of silicon carbide depend strongly on the grain boundary segregation of aluminum, which gives rise to easier deformation in high temperature creep, but also provides some toughening as a result of its association with grain boundaries. Grain boundary electrical properties are essential to ceramics used for varistor materials such as zinc oxide with added bismuth and cobalt, to positive temperature coefficient resistive materials such as many barium titanate formulations, to control of the magnetic properties of ferrite materials, and to the development of boundary layer high dielectric constant capacitors in which the grain boundaries act as an insulating layer

between semiconducting grains.

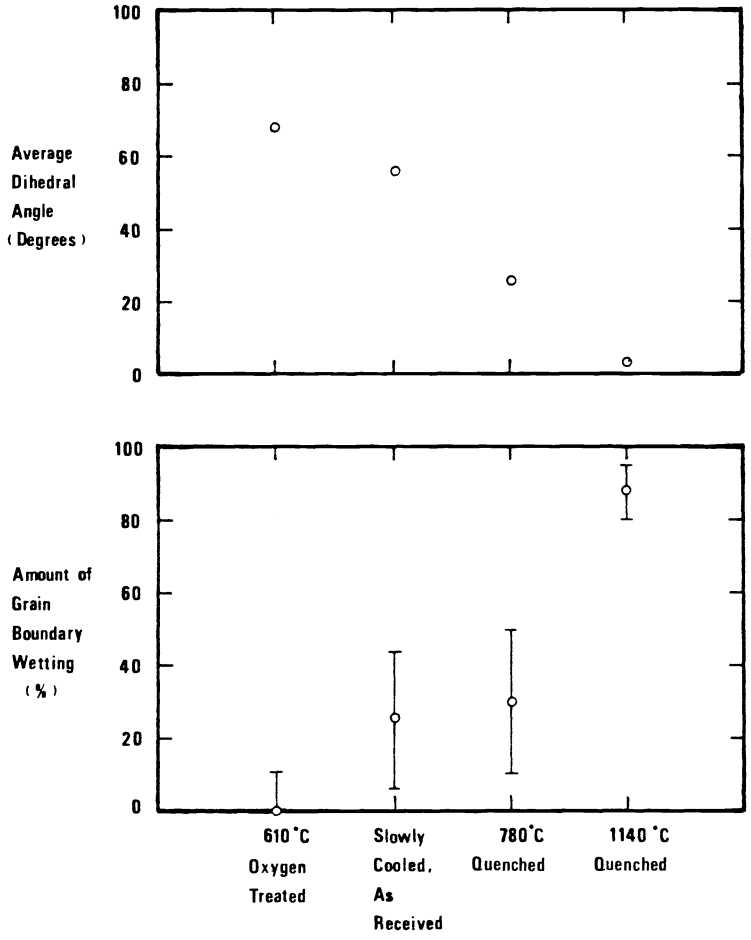

Fig. 12. Average dihedral angle (top) and the amount of grain boundary wetting (bottom) as a function of the sample heat treatment (55).

The applications of grain boundary chemistry in ceramics seems an area sure to be of increasing importance in coming years.

Acknowledgement - This work was supported by a U.S. Department of Energy grant under Contract No. DE-AC02-76ER02390.

REFERENCES

1. H. Gleiter and B. Chalmers, High-Angle Grain Boundaries, Pergamon Press, Oxford (1972).
2. Grain Boundaries and Interfaces, Edited by P. Chaudhari and J. W. Matthews, North-Holland, Amsterdam (1972).
3. The Nature and Behavior of Grain Boundaries, Edited by H. Hu, Plenum Press, New York (1972).
4. Grain Boundary Structure and Properties, Edited by G. A. Chadwick and D. A. Smith, Academic Press, New York (1976).
5. R. W. Balluffi, in Interfacial Segregation, Edited by W. D. Johnson and J. M. Blakeley, American Society for Metals, Metals Park, Ohio (1979).

6. W. A. Bollmann, Crystal Defects and Crystalline Interfaces, Springer-Verlag, New York (1970).
7. W. Bollman, "The Basic Concepts of the O-lattice Theory," Surf. Sci. 31, 1-11 (1972).
8. D. A. Smith, V. Vitek, and R. C. Pond, "Computer Simulation of Symmetrical High-Angle Boundaries in Aluminum," Acta Metall. 25[5], 475-83 (1977).
9. M. F. Ashby, F. Spaepen, and S. Williams, "The Structure of Grain Boundaries Described as a Packing Polyhedra," Acta Metall. 26[11], 1647-63 (1978).
10. R. C. Pond, D. A. Smith, and V. Vitek, "Computer Simulation of <110> Tilt Boundaries: Structure and Symmetry," Acta Metall. 27[2], 235-41 (1979).
11. J. P. Hirth and R. W. Balluffi, "On Grain Boundary Dislocations and Ledges," Acta Metall. 21[7], 929-42 (1973).
12. T. P. Danby, R. Schindler and R. W. Balluffi, "On the Interaction of Lattice Dislocations with Grain Boundaries," Philos. Mag. 37[2], 245-56 (1978).
13. J. J. Bacmann and G. Silvestre, "Structure of Near Coincidence Grain Boundaries in Germanium," to be published in Philos. Mag.
14. C. P. Sun and R. W. Balluffi, "Observation of Intrinsic and Extrinsic Secondary Grain Boundary Dislocations in [001] High Angle Twist Boundaries in MgO," Scr. Metall. 13[8], 757-61 (1979).
15. C. B. Carter and K. J. Morrissey, "Grain Boundary Structure in Al_2O_3," in Structure-Property Relationships in MgO and Al_2O_3 Ceramics, W. D. Kingery, ed., American Ceramic Society, Columbus, Ohio (1984).
16. W. D. Kingery, "Plausible Concepts Necessary and Sufficient for Interpretation of Ceramic Grain-Boundary Phenomena: 1, Grain-Boundary Characteristics, Structure, and Electrostatic Potential," J. Am. Ceram. Soc. 57[1], 1-8 (1974).
17. D. Wolf, "On the Energy of (100) Coincidence Twist Boundaries in Transition Metal Oxides," J. de Physique Colloque C6 41, C6-142-5 (1980).
18. D. Wolf and R. Benedek, Advances in Ceramics 1, 107 (1981).
19. D. Wolf, "Comparison of the Calculated Properties of High-Angle (001) Twist Boundaries in MnO, FeO, CoO and NiO with MgO," in Structure-Property Relationships in MgO and Al_2O_3 Ceramics, W. D. Kingery, ed., American Ceramic Society, Columbus, Ohio (1984).
20. D. M. Duffy and P. W. Tasker, Phil. Mag. A (1983).
21. P. W. Tasker and D. M. Duffy, Phil. Mag. Letters (1983).
22. D. M. Duffy and P. W. Tasker, "The Properties of Grain Boundaries in Rocksalt Structured Oxides," in Structure-Property Relationships in MgO and Al_2O_3 Ceramics, W. D. Kingery, ed., American Ceramic Society, Columbus, Ohio (1984).
23. G. Hesson, J. Y. Boos, I Herbeural, M. Biscondi and G. Gaux, Surf. Sci. 31 [1], 115 (1972).
24. P. Lamane and S. L. Sass, "Detection of the Expansion of a Large Angle [001] Twist Boundary Using Electron Diffraction," Scr. Metall. (1983).
25. J. Eastman, F. Schmückle, M. D. Vaudin and S. L. Sass, "Electron Diffraction and Microscopy Studies of the Structure of Grain Boundaries in NiO," in Structure-Property Relationships in MgO and Al_2O_3 Ceramics, W. D. Kingery, ed., American Ceramic Society, Columbus, Ohio (1984).
26. Alexana Roshko and W. D. Kingery (to be published).
27. Y.-M. Chiang, A. F. Henriksen, W. D. Kingery and D. Finello, "Characterization of Grain Boundary Segregation in MgO," J. Am. Ceram. Soc. 64[7], 385 (1981).
28. H. L. Marcus, ASTM Data Ser. STP 479, 90 (1972).
29. D. McLean, Grain Boundaries in Metals, Clarendon Press, Oxford (1957).
30. Ref. 52
31. Y. Tajima and W. D. Kingery, "Grain Boundary Segregation in Aluminum-Doped Silicon Carbide," J. Mat. Sci. 17, 228a (1982).
32. Y.-M. Chiang and W. D. Kingery, work in progress.
33. Chien-Wei Li and W. David Kingery, "Solute Segregation at Grain Boundaries in Poly-Crystalline Al_2O_3," in Property-Structure Relationships in MgO and Al_2O_3 Ceramics, W. D. Kingery, ed., American Ceramic Society, Columbus, Ohio (1984).
34. T. Bradley, p. 71 in Materials for Magnetic Functions, Hayden, New York (1971).
35. P. E. C. Franken, Ber. Deutsch. Keram. Ges. 55, 287 (1978) and P. E. C. Franken, H. Van Doveren, and J. A. T. Verhoeven, "The Grain Boundary Composition of MnZn Ferrites with CaO, SiO_2 and TiO_2 Additives," Ceramurgia Int. 3[3], 122-23 (1977).
36. W. N. Unertl, L. C. DeJonghe, and Y. Y. Tu, "Auger Spectroscopy of Grain Boundaries in Calcium-Doped Sodium Beta-Alumina," J. Mater. Sci. 12[4], 739-42 (1977).
37. Y. Moriyoshi, S. Shirasaki, E. S. Lee, K. Takahashi, M. Isobe, and M. Tsutsumi, "Segregation of Li_2O at the Grain Boundaries of Zinc Oxide," J. Am. Ceram. Soc. 61 [3-4], 183-84 (1978).
38. K. Uematsu, R. M. Cannon, R. D. Bagley, M. F. Yan, U. Chowdry, and H. K. Bowen, "Microstructural Evolution Controlled by Dopants and Pores at Grain Boundaries," in Proc. of International Symposium on Factors Affecting the Densification of Oxide and Non-Oxide Ceramics, Hakone, Japan, October 1978.
39. Y. W. Chung, W. J. Lo and G. A. Somorjai, "Low Energy Electron Diffraction and Electron Spectroscopy Studies of the Clean (110) and (100) Titanium Dioxide (Rutile) Crystal Surfaces," Surf. Sci. 64[2], 588-602 (1977).

40. W. D. Kingery, J. B. Vander Sande, and T. Mitamura, "A Scanning Transmission Electron Microscopy Investigation of Grain-Boundary Segregation in a ZnO-Bi_2O_3 Varistor," J. Am. Ceram. Soc. 62[3-4], 221-22 (1979).
41. U. Knauer, "Distribution of the Iron Dopant in Barium Titanate Ceramic, Determined by the Scanning Transmission Electron Microscope," Phys. Stat. Sol. (A) 53[1], 207-210 (1979).
42. T. Mitamura, E. L. Hall, W. D. Kingery, and J. B. Vander Sande, "Grain Boundary Segregation of Iron in Polycrystalline Magnesium Oxide Observed by STEM," Ceramurgia Int. 5[4], 131-36 (1979).
43. N. Mizutani, W. D. Kingery, and A. J. Garratt-Reed, unpublished work.
44. D. M. Duffy and P. W. Tasker, "A Calculation of the Interaction between Impurity Ions and Grain Boundaries in MgO," Phil.Mag., AERE Harwell Report TP.1016 (October 1983).
45. J. D. Eschelby, "The Continuum Theory of Lattice Defects," Solid State Phys. 3, 79 (1956).
46. A. H. Cottrell, Dislocations and Plastic Flow in Metals, Clarendon Press, Oxford (1953).
47. W. W. Webb, Acta Metall. 5, 89 (1957).
48. J. Lagowski, C. L. Balestra, and H. C. Gatos, "Electronic Characteristics of 'Real' CdS Surfaces," Surf. Sci. 29, 213-29 (1972).
49. J. Lagowski, E. S. Sproles, and H. C. Gatos, "Photovoltage Inversion Effect Resulting from a Continuous Spectrum of Surface States: ZnO," Surf. Sci. 30, 653-58 (1972).
50. H. C. Gatos -nd J. Lagowski, "Surface Photovoltage Spectroscopy--A New Approach to the Study of High-Gap Semiconductor Surfaces," J. Vac. Sci. Technol. 10[1], 130-35 (1973).
51. V. E. Henrich, G. Dresselhaus, and H. J. Zeiger, "Observation of Two-Dimensional Phases Associated with Defect States on the Surface of TiO_2," Phys. Rev. Lett. 36[22], (1976).
52. W. J. Lo, Y. W. Chung and G. A. Somorjai, "Electron Spectroscopy Studies of the Chemisorption of O_2, H_2 and H_2O on the TiO_2 (100) Surfaces with Varied Stoichiometry: Evidence for the Photogeneration of Ti^{+3} and for Its Importance in Chemisorption," Surf. Sci. 71, 199-219 (1978).
53. T. M. French and G. A. Somorjai, "Composition and Surface Structure of the (0001) Face of α-Alumina by Low-Energy Electron Diffraction," J. Phys. Chem. 74[12], 2489-95 (1970).
54. F. A. Kröger, Chapter 19 in The Chemistry of Imperfect Crystals, Vol. 2, North-Holland, Amsterdam (1974).
55. J. P. Gambino, W. D. Kingery, J. E. Pike, L. M. Levinson and H. R. Philipp, "The Effect of Annealing on the Microstructure and Electrical Properties of ZnO Varistors," research in progress.
56. J. D. Eschelby, C. W. A. Newey, P. L. Pratt and A. B. Lidiard, Phil. Mag. 3, 75 (1958).
57. J. Frenkel, Kinetic Theory of Liquids, Oxford University Press, New York (1946).
58. Kurt Lehovec, J. Chem. Phys. 21, 1123 (1953).
59. K. L. Kliewer and J. S. Koehler, Phys. Rev. A 140, 1226 (1965).
60. M. F. Yan, R. M. Cannon, H. K. Bowen and R. L. Coble, J. Am. Ceram. Soc. 60, 120 (1977).
61. D. M. Duffy and P. W. Tasker, "A Calculation of the Interaction between Impurity Ions and Grain Boundaries in NiO," Phil. Mag., AERE Harwell Report TP.1016 (October 1983).
62. M. F. Yan, R. M. Cannon and H. K. Bowen, "Space Charge Elastic Field and Dipole Contributions to Equilibrium Solute Segregation at Interfaces," J. Appl. Phys., 54[2], 764 (1983).
63. E. J. Verwey and J. Th. G. Overbeek, Theory of the Stability of Lyophobic Colloids, Elsevier, New York (1948).
64. M. Gouy, "Sur la Constitution de la Charge Electrique à la Surface d'un Electrolyte," J. Phys. 9, 457-68 (1910) and D. L. Chapman, "A Contribution to the Theory of Electrocapillarity," Philos. Mag. 25, 475-81 (1913).
65. S. G. Davison and J. P. Levine, Solid State Phys. 25, 1 (1970): D. R. Frankle, Crit. Rev. Solid State Phys. 4, 455 (1974) and V. Heine, pp. 228 ff. in Proceedings of the Tenth Conference Phys. Semiconductors, Cambridge, Mass. (1970).
66. O. Stern, "Zur Theorie der Elektrolytischen Doppelschicht," Z. Electrochem. 30 [21-22], 508-16 (1924).
67. N. Mizutani, A. J. Garratt-Reed and W. D. Kingery, "Grain Boundary Segregation of Iron, Chromium and Scandium in Polycrystalline Magnesium Oxide," Ceram. Int. 9[1], 31-32 (1983).
68. T. A. Yager and W. D. Kingery, "The Equilibrium Defect Structure of Iron-Doped MgO Below 1200°C," J. Mat. Sci. 16, 489 (1981).
69. M. Kinoshita, W. D. Kingery and H. K. Bowen, "Phase Separation in NiO-CoO Solid Solution Single Crystals," J. Am. Ceram. Soc. 56[7], 398-99 (1973).
70. A. F. Henriksen and W. D. Kingery, "The Solid Solubility of Sc_2O_3, Al_2O_3, Cr_2O_3, SiO_2 and ZrO_2 in MgO," Ceram. Int. 5[1], 11-17 (1979).